EFDA–JET–CP(14)01/35

G. Arnoux, J. Coenen, B. Bazylev, Y. Corre, G.F. Matthews, I. Balboa, M. Clever, R. Dejarnac, S. Devaux, T. Eich, E. Gauthier, L. Frassinetti, J. Horacek, S. Jachmich, D. Kinna, S. Marsen, Ph. Mertens, R.A. Pitts, M. Rack, G. Sergienko, B. Sieglin, M. Stamp, V. Thompson and JET EFDA contributors

Thermal Analysis of an Exposed Tungsten Edge in the JET divertor

"This document is intended for publication in the open literature. It is made available on the understanding that it may not be further circulated and extracts or references may not be published prior to publication of the original when applicable, or without the consent of the Publications Officer, EFDA, Culham Science Centre, Abingdon, Oxon, OX14 3DB, UK."

"Enquiries about Copyright and reproduction should be addressed to the Publications Officer, EFDA, Culham Science Centre, Abingdon, Oxon, OX14 3DB, UK."

The contents of this preprint and all other JET EFDA Preprints and Conference Papers are available to view online free at www.iop.org/Jet. This site has full search facilities and e-mail alert options. The diagrams contained within the PDFs on this site are hyperlinked from the year 1996 onwards.

Thermal Analysis of an Exposed Tungsten Edge in the JET divertor

G. Arnoux[1], J. Coenen[2], B. Bazylev[3], Y. Corre[4], G.F. Matthews[1], I. Balboa[1], M. Clever[2], R. Dejarnac[5], S. Devaux[6], T. Eich[6], E. Gauthier[4], L. Frassinetti[7], J. Horacek[5], S. Jachmich[8], D. Kinna[1], S. Marsen[9], Ph. Mertens[2], R.A. Pitts[10], M. Rack[2], G. Sergienko[2], B. Sieglin[6], M. Stamp[1], V. Thompson[1]
and JET EFDA contributors*

JET-EFDA, Culham Science Centre, OX14 3DB, Abingdon, UK

[1]CCFE Association, Culham Science Centre, Abingdon, Oxon, OX14 3DB, UK
[2]Institut für Energieforschung - Plasmaphysik, Forschungzentrum Jülich, Trilateral Euregio Cluster, EURATOM-Assoziation, D-52425 Jülich, Germany
[3]Forshungzentrum Karlsruhe GmbH, P.O.Box 3640, D-76021 Karlsruhe, Germany
[4]CEA/DSM/IRFM, CEA Cadarache, 13108 Saint Paul Lez Durance, France
[5]Association EURATOM-IPP.CR, Institute of Plasma Physics AS CR, Za Slovankou 3, 182 21 Praha 8, Czech Republic
[6]Max-Planck-Institut für Plasmaphysik, EURATOM-Assoziation, D-85748 Garching, Germany
[7]Association EURATOM-VR, Fusion Plasma Physics, EES, KTH, SE-10044 Stockholm, Sweden
[8]Association "EURATOM - Belgian State" Laboratory for Plasma Physics Koninklijke Militaire School - Ecole Royale Militaire Renaissancelaan 30 Avenue de la Renaissance B-1000 Brussels Belgium
[9]Max-Planck-Institut für Plasmaphysik, Teilinsitut Greifswald, EURATOM-Assoziation, D-17491 Greifswald, Germany
[10]ITER organization, Route de Vinon sur Verdon, 13115 St Paul-lez-Durance, France.
** See annex of F. Romanelli et al, "Overview of JET Results", (24th IAEA Fusion Energy Conference, San Diego, USA (2012)).*

Preprint of Paper to be submitted for publication in Proceedings of the
21st International Conference on Plasma Surface Interactions, Kanazawa, Japan
26th May 2014 - 30th May 2014

ABSTRACT

In recent melt experiments with the JET tungsten divertor, we observe that the heat flux impacting on a leading edge is 3 to 10 times lower than a geometrical projection would predict. The surface temperature, tungsten vaporisation rate and melt motion measured during these experiments is consistent with the simulations using the MEMOS code, only if one applies the heat flux reduction. This unexpected observation is the result of our efforts to demonstrate that the tungsten lamella was melted by ELM induced transient heat loads only. This paper describes in details the measurement and data analysis method that led us to this strong conclusion. The reason for the reduced heat flux are yet to be clearly established and we provide some ideas to explore. Explaining the physics of this heat flux reduction would allow to understand whether it can be extrapolated to ITER.

INTRODUCTION

Recently at JET dedicated experiments have addressed the following question: how does behave the molten tungsten in the divertor under ELM induced heat loads and what is the consequence for the plasma operations [1]. JET is the only tokamak able to produce ELMs energetic enough (300kJ) to approach conditions comparable to mitigated ELMs in ITER. An important requirement of the experiments was to reach melting transiently only (due to ELMs) and avoid any bulk melting during the inter-ELM periods. The goal of this paper is to demonstrate that this requirements has been met. Ideally this could be demonstrated with an accurate measurement of the lamella surface temperature. The temperature measured with an infrared (IR) camera [2] provides only a partial information because of its limited resolution and its partial coverage of the lamella. In this paper we expose an analysis method that allows to retrieve the temperature distribution of the lamella combining a 3D thermal simulation and a set of experimental measurements. After a description of the experimental setup, one describes the IR measurements, its limitations and the method we developed to retrieve a "true" temperature. This method allowed us to demonstrate with a high degree of confidence that the heat load reaching the side of the lamella is lower by at least a factor 2 than that obtained with a geometrical projection of the heat flux parallel to the magnetic field lines, $q_{||}$.

1. EXPERIMENTS AND EXPERIMENTAL SETUP

The JET bulk W divertor outer target is composed of 96 tiles. Each tile is made of 4 stacks, composed of 24 lamellas (Figure 1). One lamella is typically 40mm high by 58mm long by 5mm wide. For the purpose of the melt experiments one tile was modified. The inner most stack (stack A) was designed to expose the side of a tungsten lamella. The height of the exposed edge varies from 0.25mm at the low field side (LFS) up to 2.4mm at the high field side (HFS). The heat load on the side of the lamella is about 30 times higher than that on the top due to the shallow angle that the magnetic field lines make with the top surface. Exposing the side facilitates the access to near melting temperatures and melting induced by ELMs, while ensuring the integrity of the rest of the diverter target. A plasma scenario was carefully developed with a strike point movement from

stack B to stack A in order to control the duration of the exposed lamella. The melting scenario is an H-mode plasma with plasma current I_p = 3MA, input power, P_{in} = 23MW, and with low gas rate fueling ($0.55 \cdot 10^{22}$ e$^-$/s) in order to achieve large, regular ELMs.

Figure 2 shows a schematic representation of the lamella, the local frame of reference $\{x'; y'; z'\}$ in the context of the usual tokamak cylindrical coordinates, $\{R; \phi; z\}$, and the heat load distribution on both the standard and special lamellas. For the normal lamellas, the heat flux reaches only the top surface ($q_s = 0$) since the side is shadowed by its neighbor. In that case, the heat diffuses from the top, mainly in the depth of the tile (z'), toward the heat sink (tile carrier). The heat also diffuses in the poloidal (x') direction because of the non uniformity of the heat load distribution along the lamella. In the toroidal direction, the flux can be considered as uniform and the heat diffusion problem can therefore be simplified to a 2D problem. This simplification is not possible on the special lamella where $q_s >> q_n$. The highly non uniform heat loads on the side of the lamella generate very strong temperature gradients in both the depth (z') and toroidal (y') directions (typically $\nabla_{y'} T = 400^o$C/mm in steady state and it is even stronger during transients loads). These strong gradients cannot be resolved with our IR camera and we developed a complex method to retrieve the temperature distribution of the lamella.

2. MEASUREMENTS AND METHOD

As illustrated in Figure 3 the field of view of the IR camera covers the top surface of several lamellas. In this paper we focus our attention onto two lamellas: the special lamella, $T_n(x', y', t)$, and a reference lamella, $T_n^A(x', t)$ (labelled A in Figure 3). $T_n(x', y', t)$ is decomposed in the y' direction, into 8 rows of 30 pixels each, corresponding to poloidal (x') slices (slice H to O in Figure 3 (a)). The peak temperature, $T_{n,peak}(t)$, on the special lamella is strongly underestimated because the pixel resolution of the camera (1.7pixels/mm) cannot resolve $\nabla_{y'} T$. (Note that the resolution was optimised to resolve typical poloidal temperature profiles and $\nabla_{x'} T << \nabla_{y'} T$). The example in Figure 3 (b) illustrates that the peak temperature inter-ELM can typically be underestimated by $500^o C$. During ELMs we will show (Figure 5) that the peak temperature increase, $\Delta T_{peak,ELM}$ is typically underestimated by a factor 7 (when one mesures $\Delta T_{peak,ELM} = 180^o$C, it actually means $\Delta T_{peak,ELM} = 1400^o$C).

In order to retrieve the real peak temperature of the lamella, which ultimately determines when it melts, we developed a complex analysis procedure in 4 main steps. 1) One determines the heat load poloidal profiles, $q_n(x', t)$, using the temperature profiles, $T_n^A(x', t)$ measured on the reference lamella. 2) The $q_n(x', t)$ signal is conditioned and $q_s(x', t)$ is determined based on the local geometry of the magnetic field. 3) The two signals are used as an input into the MEMOS code and the outputs are analysed. 4) The MEMOS outputs are processed to simulate synthetic measurements, which are compared with the real measurements. The rest of this section describes in more details those four steps.

2.1. STEP 1)

$q_n(x',t)$ is derived from $T_A(x',t)$ using the THEODOR code. This is a standard procedure used in many JET divertor IR analysis (See for example [3]). For our melting pulse scenario, we verified that the typical ELM peak energy fluency, $\varepsilon_{elm,peak} = 150$ kJ/m^2 is consistent with the pedestal pressure, P_{ped} = 7 kPa (measured with a high resolution Thomson scattering system) as predicted by the scaling proposed by Sieglin et al [3].

2.2. STEP 2)

The data conditioning consists of smoothing the profile $q_n(x',t)$ (in the x' direction for each time slice) using a fit function thereby reducing the noise inputs into the MEMOS code. Figure 4 shows a profile, $\langle q_n(x')\rangle_t$ and the resulting fit, $\langle q_{n,fit}(x')\rangle_t$, time averaged over one inter-ELM (20ms) and one ELM (1ms) period. The shape of $\langle q_n(x')\rangle_t$ during the inter-ELM period is unusual with no apparent strike point (no decay in the private flux region is observed). Our initial interpretation was that it is an artefact and we decided to force the fit to zero in the PFR, resulting in the red profiles with a peak heat flux about 3 times smaller (about 4MW/m^2 instead of 12MW/m^2). This interpretation was reinforced by the fact that we could not get consistent melt motion simulations with the original profiles. The ELMs are fairly well reproduced by our fit. From $q_{n,fit}(x',t)$, one infers the heat load on the side of the lamella, $q_{s,fit}(x',t) = \eta_q(x',t) \cdot q_{n,fit}(x',t)$ where $\eta_q(x',t) = 1/\tan(\theta_\perp(x',t))$. $\theta_\perp(x',t)$ is the field line angle with the top surface of the lamella: $\tan(\theta_\perp) = B_N/B\phi$ with $\mathbf{B}_N = (\mathbf{B}_R + \mathbf{B}_z) \cdot \mathbf{N} \cdot \mathbf{N}$ and $\mathbf{N}$ the normal vector to the lamella surface. In our case $\theta_\perp$ typically increases linearly from 1.5^o at $x' = 0$ (HFS) to 2.5^o at $x' = 58$mm (LFS), which corresponds to $30 \geq \eta_q \geq 20$. Note that this definition of η_q assumes that the lamella surface is horizontal in the toroidal direction. In reality, the stack is tilted by $\alpha_s = 0.5^o$ and $\eta_q = \cos(\theta_\perp + \alpha_s)/\sin(\theta_\perp + \alpha_s)$. Here we neglect α_s implying that $q_{s,fit}$ is slightly undervalued, but no more than 30%.

2.3. STEP 3)

The MEMOS code simulates the thermal diffusion into the lamella, the dynamic of the 3 phases of tungsten (solid, liquid and vapour), how they interface with the plasma and how the liquid and vapor move. It is worth noting that amongst the cooling process of the lamella are included the W vapor shielding and thermoelectric emission of electrons. For more details on MEMOS see [4]. In order to benchmark the MEMOS simulations we compare 3 quantities with the measurements: i) The W vaporisation rate, W_{vap} [atom/s], which is also deduced from the WI line emission measurements, emitted from the lamella (we assume that all the W atoms vaporized from the lamella emit in that line before they escape the volume viewed by the spectrometer, typically 150cm^2 projected onto the target). ii) the maximum depth of molten tungsten per JET pulse, which is evaluated from a high resolution photography taken of the lamella after each melting pulse. After a total of 5 melting pulse, with high reproducibility [1] it was evaluated that about 1mm (in the y' direction) of material was removed from the corner of the lamella for a total of 6 to 7mm^3 of material moved/vaporised, that

is to say 200μm per pulse. iii) We are ultimately interested in the peak temperature and its location on the melted lamella. The hottest point on the lamella is always on the corner ($y'= 0$ and $z'= 0$), but the poloidal temperature distribution varies. Typically, the peak temperature during ELMs and inbetween ELMs is not at the same location so we focus our attention on $T_{MEMOS}(x', y'= 0, z'= 0, t)$ as illustrated in red in Figure 5 (e) and (f). The comparison with the measurement is not immediate and the MEMOS results must be processed in order to simulate the resolution of the IR camera.

2.4. STEP 4)

From the top surface temperature map, $T_{MEMOS}(x', y', t)$ (150×104 grid), one simulates the IR camera measurements, $T_{sim}(x', y', t)$ (150×4 grid), by applying an instrumental function transformation [5]. $T_{MEMOS}(x', y', t)$ is converted into a luminance map, $I_{MEMOS}(x', y', t)$ using the Planck radiation function. The grid resolution of $I_{MEMOS}(x', y', t)$ is reduced to that of $I_{sim}(x', y', t)$ by averaging the intensity and convoluting with the pixel leakage function. In our case one pixel intensity is modeled by a gaussian profile of half width at half maximum σ = pix / 2 [5]. $T_{sim}(x', y', t)$ is derived from $I_s im\ (x', y', t)$ and an example of $T_{sim}(x', y' = 0)$ is shown in Figure 5 (e) and (f) for a time before an ELM and the peak of an ELM respectively.

3. RESULTS AND DISCUSSION

The MEMOS simulations and the measurements are compared in Figure 5. T_{MEMOS} (in black in Figure 5 (b)) suggests that the lamella was melted instantly with a near bulk meting around $t = 13.2$s. For this simulation, the corresponding W_{vap} is two order of magnitude higher than that measured (Figure 5 (c)). The much higher vaporisation rate translate into a depth of melted material of about 450 μm per pulse, which is more than 2 times higher that what is measured. This suggests that the $q_s(x', t)$ applied into the MEMOS simulations is far too high.

Our approach here is to apply a reduction factor f_s in the calculation of q_s such that $q_s = f_s \cdot \eta_q \cdot q_n$, with $0 < f_s < 1$. Several iterations were required to converge to the best case with $f_s = 0.4$. In that case Figure 5 (d) shows a fair agreement of W_{vap} between the simulation and the measurement, with a melted depth of 200μm, as measured. The temperature profiles show a very good agreement, at least in the SOL ($x' > 20$ mm) for both the inter-ELM (Figure 5 (e)) and the ELM (Figure 5 (f)) phases. The good agreement of 3 independent measurements and the fact that the simulated temperatures are in fair agreement with the measurement show that the melting was induced by transients only, since the inter ELM temperature simulated (red temperature in Figure 5 (b) does not cross the melt threshold. Note that the disagreement between the simulated temperature and the measurement in the private flux region is due to the constraint we put on the fitted profiles. We also note that W_{vap} in the simulation is higher a the beginning of the pulse and get in better agreement near the end of the pulse. This suggest that f_s is probably not constant in time. We actually now believe that the measured profiles are real and that the strike point inter-ELM is actually out of the tile. In order to obtain the correct temperature distribution and consistent melt motion in the simulation, we would

have to use a different heat flux reduction factor during and between ELMs: $f_{s,ELM}$ and $f_{s,inter-ELM}$.

The question is then why do we need f_s? Is it real or is it a measurements artefact. The latter can be ruled out. One could argue that q_s is too high because q_n is overestimated. We have verified that q_n is consistent with measurements in other experiments (e.g. $\varepsilon_{peak,elm}$ scales with P_{ped} as in [3]) and that a reasonable energy balance is obtained. We also investigated the effect of the finite Larmor radius, ρ_L, that smoothes the power load if the height of the exposed edge, h, is of comparable size as ρ_L (this is the case during ELMs). Particle in Cell simulations show that this would reduce the heat load by at most 25% [6] during ELMs. It might play a role during ELMs but it does not explain the need of f_s between ELMs. Note that $f_s \simeq 0.2$ is necessary in L-mode plasmas, where $\rho_s << h$ and where the lamella temperature is far from melting conditions. The causes of this missing heat load are a matter of future investigations but it is potentially a positive results for ITER as the leading edges might not be as vulnerable as one might think. It is however premature to be fully conclusive and further work is need to understand the physics reason of this missing flux. One could speculate that the specific geometry of the modified stack generates local turbulence that enhance the perpendicular transport. The fact that we probably need a lower f_s inter-ELM than during ELM point in favor of that speculation.

CONCLUSION

A careful analysis of the thermal response of a W lamella reaching melting conditions in the JET divertor has been carried out. We have demonstrated that the lamella was melted by ELM induced heat loads only. Our analysis compares the simulations of the MEMOS code with our measurements. In this analysis we demonstrate that the heat loads reaching the exposed edge of the melted lamella is at least half (a global reduction factor of 0.4 is required) of that predicted by the geometrical flux enhancement factor. The analysis method requires some refinement, in particular a different reduction factor for the ELM and inter-ELM phases. This suggest that the local transport in front of the exposed edge might be enhanced during inter-ELMs and this will be investigated in a future work. It is essential to understand the nature of this reduction as it could potentially have beneficial effect for ITER.

ACKNOWLEDGEMENT

This work, part-funded by the European Communities under the contract of Association between EURATOM/CCFE was carried out within the framework of the European Fusion Development Agreement. For further information on the contents of this paper please contact publications-officer@jet.efda.org. The views and opinions expressed herein do not necessarily reflect those of the European Commission. This work was also part-funded by the RCUK Energy Programme [grant number EP/I501045]

REFERENCES

[1]. J. Coenen et. al. This conference, **I8**, 2014.

[2]. I. Balboa et al. Review of Scientific Instruments, **83**:10D530, 2012.

[3]. B. Sieglin et al. Plasma Physics and Controlled Fusion, **55**:124039, 2013.

[4]. B. Bazylev et al. This conference, **P2-098**, 2014.

[5]. Y. Corre et al. This conference, **P3-086**, 2014.

[6]. R. Dejarnac et al. Nuclear Fusion, Submitted for publication, 2014.

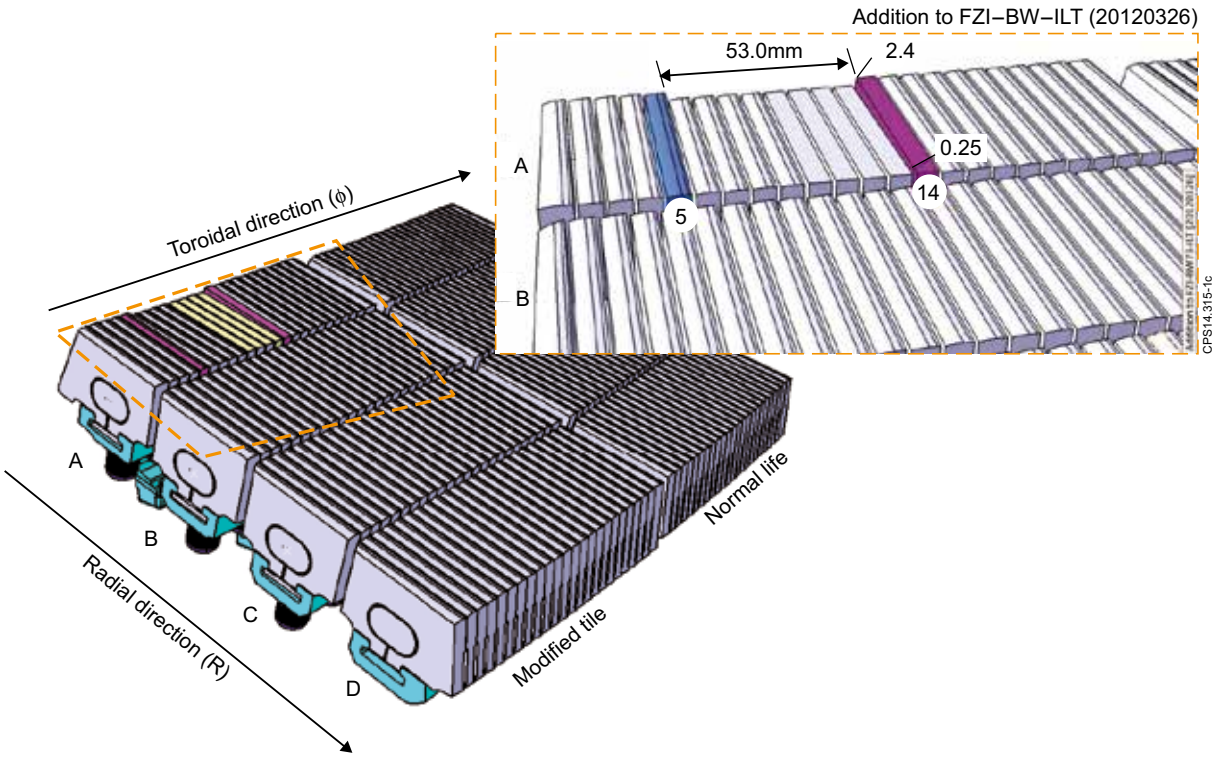

Figure 1: Drawing of the JET divertor outer target module with its modified stack. The insert shows details of the lamellas arrangement in the modified stack A, with the exposed side of lamella number 14 (purple).

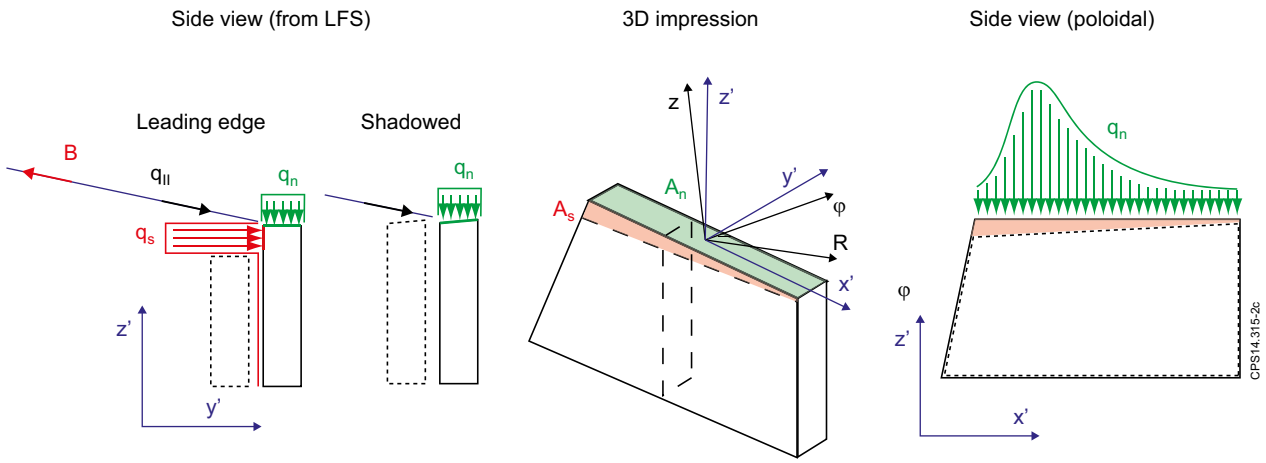

Figure 2: Schematic representation of the typical heat loads distribution on both the special and normal JET divertor lamellas. Both the local frame of reference: {x'; y': z'} of the lamella and the classic cylindrical coordinates: {R; ϕ ; z} are defined. Note that x'is in the poloidal plane, defined by R and z. The heat loads is decomposed into two components: the heat load profile on the side, q_s, and on the top, q_n, of the lamella.

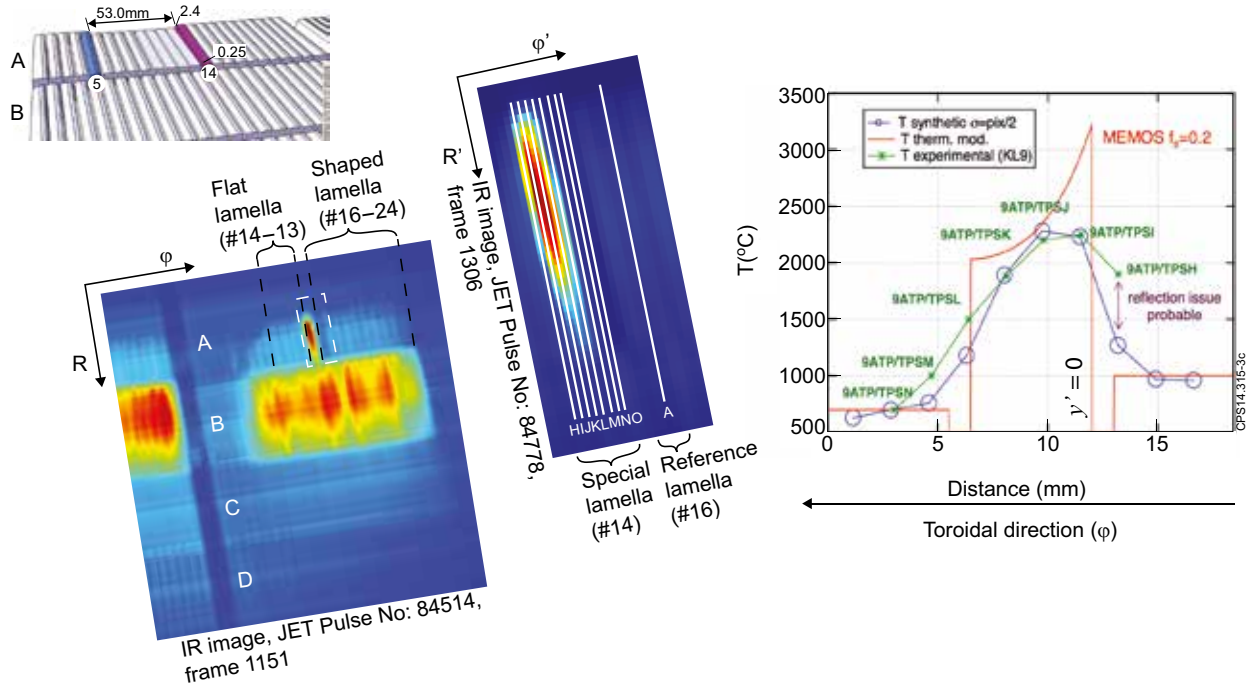

Figure 3: Example of the IR camera field of view with the special lamella clearly hotter than the others. The Special lamella surface is covered by 8 rows of 50 pixels (labelled H to O) and can be compared with a reference lamella (labelled A). An example of a typical toroidal temperature profile measured by the IR camera is compared with a simulated measurement inferred from the profiles predicted by the MEMOS simulations. This illustrates how much the measurements underestimate the temperature (the pixel resolution cannot resolve the temperature gradient).

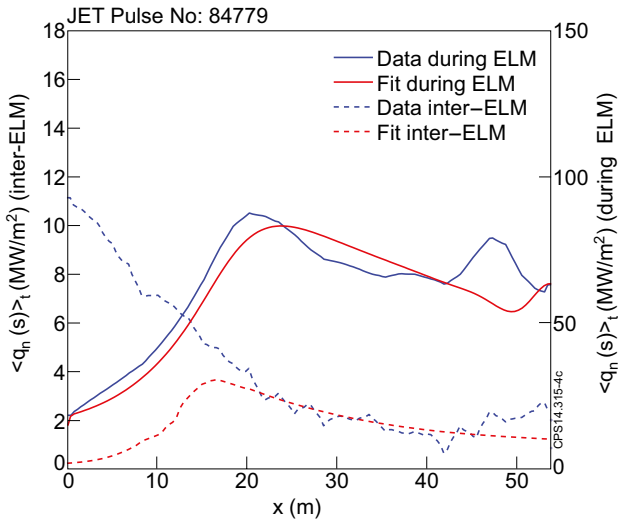

Figure 4: Typical time averaged heat load profile, $\langle q_n(x')\rangle_t$ for an inter-ELM, t = [13.85 : 13.87]s (dashed) and ELM, t = [14.174 : 14.1775]s (plain) periods. In blue is shown the measurement and in red is the fitted data used for inputs into the MEMOS code.

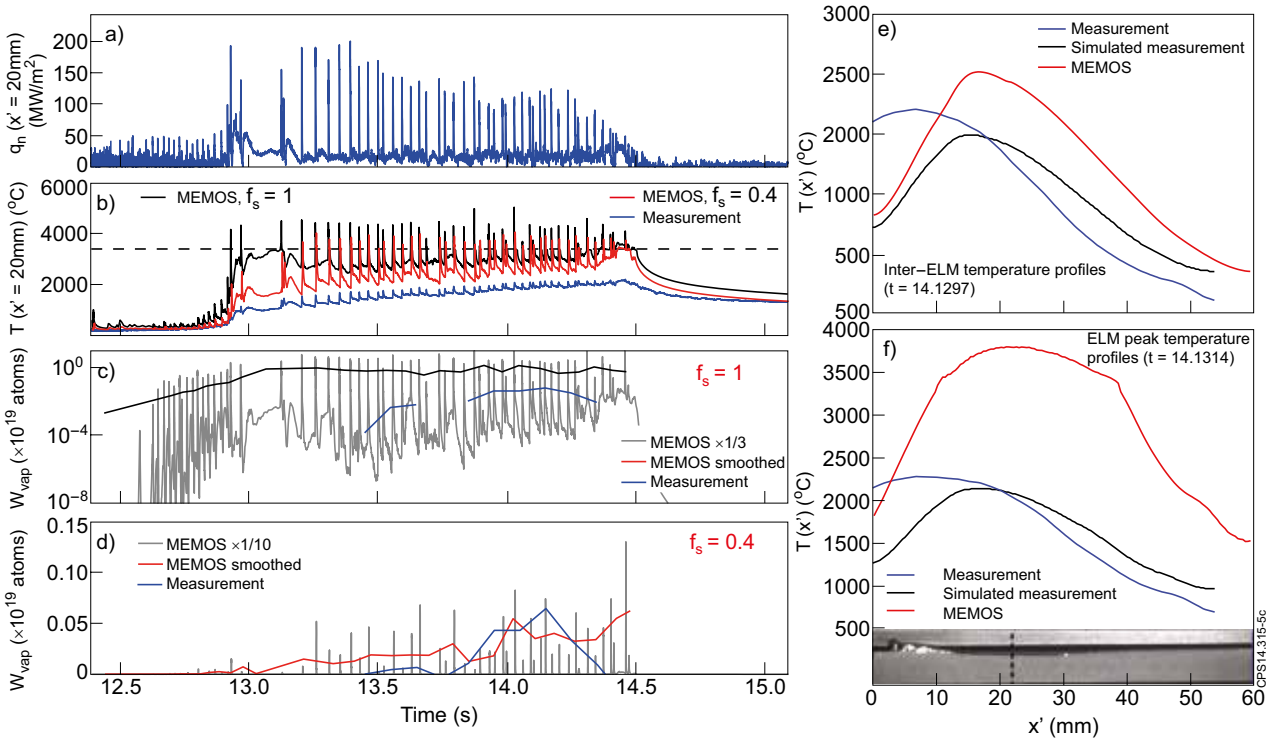

Figure 5: Time evolution of the measured peak heat flux on the reference lamella, $q_{n,peak}(t)$ (a), the measured and simulated (MEMOS) peak temperature of the melted lamella, $T_{peak}(t)$ (b) and the measured and simulated W vaporisation rate for two different heat flux reduction factor, $f_s = 1$ (c) and $f_s = 0.4$ (d). In (b) the simulated temperatures are shown for both $f_s = 1$ (black) and $f_s = 0.4$ (red). The original simulated W_{gap} in (c) and (d) is time averaged over 200ms to simulate the measurement (exposure time of the spectrometer), leading to the black (c) and red (d) traces. (e) and (f) temperature profiles before and at the peak of an ELM respectively, measured (blue), simulated by MEMOS (red) and simulated measurement from MEMOS (black). In (f) a big resolution picture of the melted lamella is inserted and the dashed line indicate the deepest, reference melt thickness.